

Transition to stress focusing for a thin elastic sheet locally curved

Thomas Barois, Ilyes Jalisse,¹ Loïc Tadrif,² and Emmanuel Viot³

¹Univ. Bordeaux, CNRS, LOMA, UMR 5798, F-33400 Talence, France

²Aix Marseille Univ, CNRS, ISM, Marseille, France

³hap2U, 75 Avenue Gabriel Péri, 38400 Saint Martin d'Hères, France

A rectangular thin elastic sheet is deformed by forcing a contact between two points at the middle of its length. A transition to buckling with stress focusing is reported for the sheets sufficiently narrow with a critical width proportional to the sheet length with an exponent $2/3$ for the limit of small thicknesses. Additionally, a spring network model is solved to explore the thick sheets limit and to validate the scaling behaviour of the transition for the thin sheets limit. The numerical results reveal that buckling does not exist for the thickest sheets and a stability criteria is established for the buckling of a curved sheet.

The crumpling of a paper sheet is an usual outcome for someone trying to write a deep and meaningful piece of text such as the introduction of a scientific paper. After being crumpled, the paper is irreversibly damaged and its topography may be viewed as a disordered network of ridges. The persistence of such ridges is a structural memory of stresses focused during the forced manipulation of the paper sheet.

Developable deformations of pure bending should prevail for thin sheets due to the large mismatch between thickness and typical size[1]. To understand crumpling, a notable situation of non-developable deformation, stress focusing[2] is an essential concept. Stress focusing is obtained in model experiments like the indentation of a thin plate against a circular contour[3–5]. The resulting structure is called a developable cone (or d-cone[6]) and it conveys the idea that the plate adopts a conical shape in order to satisfy developability. Experimental d-cones do not rigorously match with conical surfaces. A U-shaped scar is found at the tip of a d-cone. The formation of this scar is the consequence of the sheet locally avoiding diverging curvatures at the apex of the cone. This picture of stress focusing can be generalized to crumpling[7–12]: a crumpled configuration is a state occupying a small volume that combines regions approaching developability and localized ridges focusing the stretching deformations.

In all the previous situations reported, a confinement is imposed to a thin sheet and stress focusing is compulsory because there are no developable deformations that can be contained within the imposed volume. In this work, we identify the existence of a transition to stress focusing for a thin sheet submitted to a pure bending deformation. This result shows that structural buckling can be observed for a thin sheet without an imposed volume condition. The main outreach of this work is about the fundamental understanding of crumpling dynamics with the identification of a class of crumpling precursors appearing while solutions of pure bending could satisfy to the boundary conditions. A second outcome is the characterization of the buckling threshold. This has a practical interest for the safe handling of a piece of thin material without inducing stress focusing that would result in

structural damages[13, 14]. The characterization of this transition is also of interest in a context of exploiting buckling and crumpling for the realization of functional and smart materials[15–21].

The point of this work is to evidence a route to crumpling by the only forcing of low-energy bending modes without *a priori* forcing of the stretching modes of much higher elastic energy. Forcing the bending modes could be viewed as a one direction confinement. Stress focusing can be observed for one direction confinement but with peculiar boundary constraints such as an imposed 3-buckle shape[22] or a pulling force[23]. In other situations with frames imposing boundary constraints, the transition to stress focusing can be reversed and defects can appear at small confinement before developable[24] or smooth[25] solutions establish for larger external load or compaction. In the case of draping[26], a transition to stress focusing exists for a soft sheet bent under its own weight but this transition is assisted by the supporting tip that adds a localized stress.

The present study is based on a simple self-contact procedure applied to a thin sheet in order to characterize the transition to stress focusing. Figure 1 (a) represents a rectangular elastic sheet of length L and width W . The thickness t is small compared to W and L . The material coordinates of the sheet u, v verify $u = x$ and $v = y$ for the sheet flat. Any configuration of the sheet can be formally described by $x(u, v)$, $y(u, v)$, $z(u, v)$. The origin of the frame xyz is taken at the center of the sheet.

The procedure consists in putting in contact the two points at the mid-length of the sheet $u = 0$ marked by square symbols in figure 1. In the same figure, snapshots of two elongated sheets are shown for (b) a small ($L/W \approx 2$) and (c) a large aspect ratio ($L/W \approx 6$).

For the aspect ratio $L/W \approx 2$, the sheet is transversely curved without stress focusing. The sheet is however not free of stretching deformation and the presence of a small longitudinal stretching is responsible for the symmetric opening of the curved sheet. This coupling between transverse bending and longitudinal stretching is known to establish a finite persistence length for the curved region[27–33]. The limit for a sheet free of stretch-

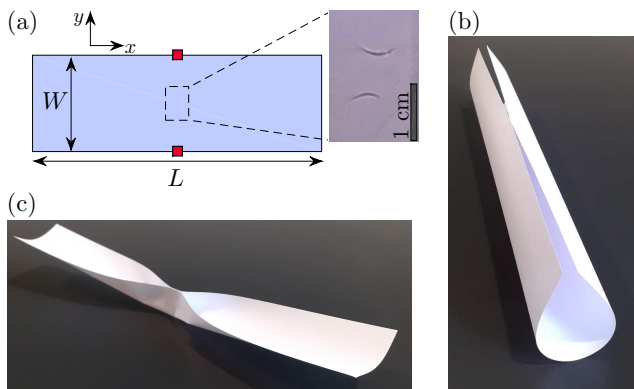


FIG. 1. (a) Schematics of a flat sheet of width W and length L . (u, v) are the material coordinates of the sheet that match with (x, y) for the flat sheet. The square markers indicate the mid-length points. A picture is inserted showing the scars formed after a self-contact procedure with an acetate sheet ($L = 29.7$ cm, $W = 8$ cm, $t = 0.2$ mm) (b) Photograph of a rectangular paper strip ($L = 29.7$ cm, $W = 15$ cm, $t = 0.1$ mm) with mid-length points at contact and maintained by an adhesive strip. (c) Photograph for a strip with a smaller width ($L = 29.7$ cm, $W = 5$ cm, $t = 0.1$ mm).

ing would be obtained for a small length $L \ll W$. In this case, the sheet profile would be invariant along x and it would match with Euler's elastica[34] model in the projection plane yz . This limit allows to identify a developable solution with a finite elastic energy for any sheet size that would satisfy the boundary condition of the two points at contact: for any set of dimensions L, W, t , a developable surface can be obtained from an elastica profile in the plane yz invariant in the direction x .

For the large aspect ratio L/W , the morphology of the sheet is modified and the stress focusing results in the formation of persistent scars close to the mid-line $u = 0$. The inserted picture in figure 1 (a) shows the two scars resulting from the nucleation of two d-cones observed in an acetate sheet of dimensions $L = 29.7$ cm, $W = 8$ cm and $t = 0.2$ mm after self-contact. For the paper sheet in figure 1 (c) four d-cones are formed. In this case, L/W is larger than for the acetate sheet. This points towards a route to crumpling with an increasing disorder for the sheets of large ratio L/W . Here, the experiments are purposely performed close to the transition region and the post-buckling morphology does not show the usual ridges network[35] as for strongly confined sheets.

The appearance of stress focusing for a sheet simply curved, even locally, is certainly counter-intuitive because the bending modes have an elastic energy orders of magnitude below the stretching modes. If one consider $W = 5$ cm for typical scale of the buckled sheet in figure 1 (c), the ratio for the bending energy to the stretching energy linearly coupled is $(t/W)^2 \sim 4 \times 10^{-6}$. Stress focusing is even more surprising in this context since bending is usually considered as a strategy to protect thin

sheets from collapse under external loads according to the concept of *curvature-induced rigidity*[31, 33].

A possible explanation for the occurrence of stress focusing in the present experiments could simply be the result of a careless manipulation of the sheet during the self-contact procedure (unintentional poking, unwanted gravity load, ...). This careless manipulation hypothesis would be expected for the very thin sheets for which manipulation without stress focusing is a challenge, like it is for example for the manipulation of a thin aluminum foil for a kitchen use.

To rule out the careless manipulation hypothesis, a set of experiments is performed with acetate sheets ($t = 0.2$ mm) to identify a reproducible transition to stress focusing. Figure 2 presents a diagram that gives the state of a sheet with mid-length point contact as a function of the reduced variables L/t and W/t . The diagram has an aspect ratio 2:1 and it compares experimental results (data points) with numerical simulations (gray background). The numerical results are obtained with a spring-network model that will be discussed further. A postcard and a metro ticket are shown on the diagram to get a sense of the orders of magnitude without the corresponding experiments being actually performed.

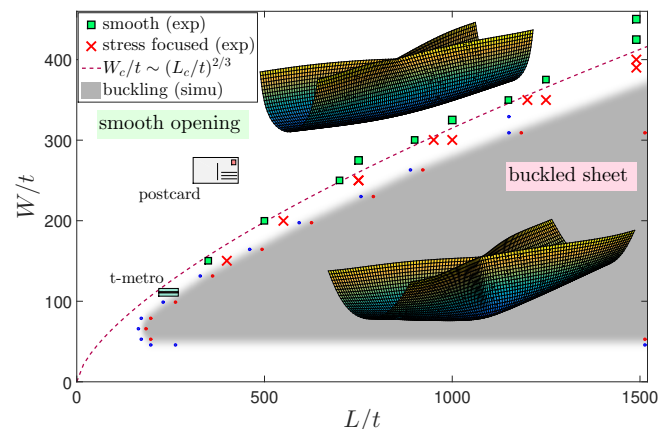


FIG. 2. State diagram of a thin sheet with mid-length points contact (L : length, W : width). The data points are for experiments with acetate sheet (thickness $t = 0.2$ mm) with squares for a sheet opening smoothly and crosses for sheets with stress focusing. The dashed line is a power-law with an exponent $2/3$ and a numeric prefactor 3.15. The gray area indicates a stress focusing region obtained from the simulation of a spring network model. A representation of two simulated sheets ($W = 200$) is presented with $L = 500$ for the smooth opening and $L = 550$ for the opening with focused stresses. The dimensions of a metro ticket and a standard postcard are indicated. The data point for an A4 paper is well outside the plot ($L/t \sim 3000$, $W/t \sim 2000$), in the smooth opening region.

For the experimental set with the data points, the transition to stress focusing occurs in a region with sufficiently large value of L/t for a fixed W/t . The small-

est width explored is $W = 3$ cm which corresponds to $W/t = 150$. For this value, the bending deformation for the mid-length contact points is such that the sheet enters in a plastic deformation regime, which is out of the scope of this work. The largest width explored is $W = 9$ cm, slightly above the width for the transition for a sheet of length 29.7 cm ($L/t = 1485$) cut from a standard A4 format. The dashed line is a scaling law $W_c/t = a(L_c/t)^{2/3}$ with the adjustment $a = 3.15$. The exponent of the scaling law is smaller than one which means that, in the limit $t \rightarrow 0$, the sheet is without stress focusing. Along with the existence of a scaling law, the absence of crumpling for the thinner sheets with low stiffness proves that the buckling transition observed is not the result of unintentional loads.

In order to explore the validity of the scaling exponent, notably for the thick sheets with W/t and L/t relatively small, a spring-network model is computed. Although crystalline spring networks do not rigorously model the isotropic elasticity of continuum media[35–39], such models are well adapted to explore the scaling properties of thin sheet configurations[40]. Figure 3 (a) presents the structure of the unit cell used in the simulation with linear springs of length unity for the first neighbors and springs of length $\sqrt{2}$ for the second neighbors. A thin sheet is obtained by 2D-replication of the unit cell to form a bi-layer of vertices linked by an ensemble of springs. First, a flat sheet is generated and then additional springs are added and tuned to force the contact between the mid-length points. The equilibrium positions of the vertices are computed by iteration of the spring forces until a static equilibrium is found (see Supplemental Material, II.D.). The spring network model is without gravity.

The spring network model is computed for different sheets dimensions to identify the transition between a smooth opening and a buckled sheet with focused stresses. The criteria to identify a buckled sheet is the sign of the transverse curvature. With a smooth opening, the transverse curvature is always positive. For a buckled sheet, the transverse curvature is partly negative at the middle of the sheet $u = 0$. Figure 2 represents a filled area corresponding the parameters domain with focused stresses. The area for stress focusing is identified up to $W/t_e \approx 330$, for the largest sheet computed with $1851 \times 471 \times 2$ vertices. Although the thickness of the bi-layer is one, its effective thickness for the bending rigidity is $t_e = 1.52$. This comes from the fact that the springs are not uniformly distributed within the sheet thickness but only at the top and bottom layer, where the bending moment is higher. The calibration of t_e is detailed in the supplemental material.

Stress focusing is not observed in simulations below $W/t_e = 56$. For $W/t_e < 56$, the simulations indicate that an elastic sheet can open smoothly until the persistence length for the transverse curvature is reached. In this regime, there is no risk of damages by stress focus-

ing during manipulation and self-contact. This regime is however difficult to explore with thin elastic sheets. With paper ($t \approx 0.1$ mm), it would require to use strips with W of the order of 5 mm. For such narrow strips, it is not possible to force a self-contact without entering in the plastic regime.

The regime of focused stresses is observed for a larger range of parameters in the experiments compared to the simulations. This systematic difference could be explained by the difficulty to realize controlled experiments with thin sheets. Because the mechanical properties of thin sheets are never perfectly uniform, experimental buckling is expected below an ideal sheet perfectly homogeneous. To illustrate this, a set of experiments was performed with standard paper and the transition was found for lower L/t_e than the transition for the acetate sheet (not shown in figure 2 for clarity, see Supplemental Material, I). This observation is consistent with the fact that paper is a fiber-based material[41] less homogeneous and with more anisotropy than acetate sheets. Another difficulty in the experiments is the contact procedure that needs to be performed carefully to avoid an excessive stress when approaching the two mid-length points that could ease the buckling transition.

The results of the simulations are further processed to investigate a criteria for the sheet buckling under self-contact. Figure 3 (b) represents the longitudinal strain profile ϵ_{uu} for a sheet of $1800 \times 470 \times 2$ vertices ($L/t = 1184$, $W/t = 309$) with contact of the mid-length points. The strain profile is obtained during the simulated dynamics of the sheet, just after the buckling event. A video (see Supplemental Material, III.) shows the evolution of the sheet configuration and the strain profile during the simulation iteration process. The strain profile combines regions of positive stretching, to allow the sheet to open, and regions of negative stretching (compression). The existence of compression with the opening of a curved strip was pointed out in a previous work[30] and it can be viewed as a consequence of the mechanical equilibrium of the longitudinal stress integrated over the width of the strip. There are 4 points of maximal compression lying at the middle of the compression bands and longitudinally separated by a distance δ . For a post-buckled sheet, each point of maximal compression is the source point of a d-cone structure.

Figure 3 (c) represents the value of the maximal compression strain $\min(\epsilon_{uu})$ for a sheet as a function of the width W/t_e . The strain is normalized with the dimensionless factor W/t_e . Each data point corresponds to a unique couple (W, L) and the length L of the sheets is indicated by a horizontal bar for each data point. The plot shows two families of data points: the circle scatters are for the smooth sheets, without curvature inversion, and the square or star scatters are for the post-buckled sheet with curvature inversion of the transverse profile (see inserted schematics). The data point with a star

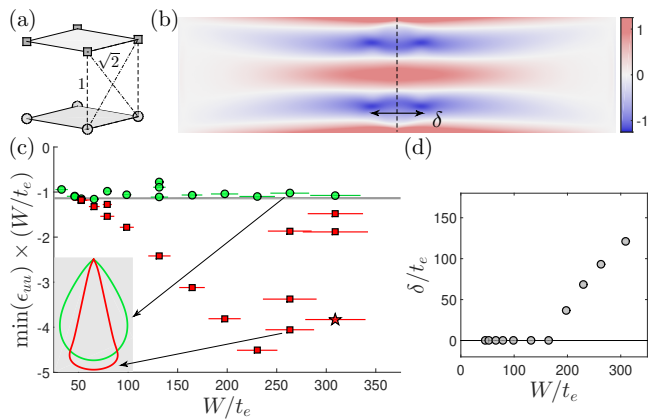


FIG. 3. (a) Unit cell of the spring network model. Circles and squares represent the lower and the upper surface. The linear springs of length 1 and $\sqrt{2}$ are for the first neighbours and the second neighbours vertices respectively. (b) Normalized longitudinal strain $\epsilon_{uu} \times (W/t_e)$ of a simulated sheet ($L = 1800$, $W = 470$) just after buckling. The dashed line is the mid-line $u = 0$. Positive values corresponds to a stretching and negative values are for a compression. 4 points of stress focusing are present. (c) Normalized minimal strain $\min(\epsilon_{uu})(W/t_e)$ (compression) as a function of the dimensionless width W/t_e . The circles are for simulated sheets with smooth opening and square symbols are for sheets with stress focusing. The horizontal line is at -1.16 . The profile at mid-length $u = 0$ illustrates the curvature sign change with buckling. The star symbol indicates the sheet ($L = 1800$, $W = 470$) selected for the strain profile represented in (b). $t_e = 1.52$. (d) Horizontal spacing of the local minima for the longitudinal strain.

corresponds to the dimension for the strain map in figure (b).

The plot in figure 3 (c) suggests the existence of a threshold value $\min(\epsilon_{uu}) \times (W/t_e) = -1.16$ below which a sheet at self-contact buckles. The buckling dynamics can be followed in more details with the successive profiles of the sheet during the simulation. A plot is provided in Supplemental Material (Fig. S8) that represents the evolution of the maximal compression strain during the convergence of the mechanical equilibrium of the simulated sheet. The sheet with $1700 \times 470 \times 2$ vertices ($L/t = 1118$, $W/t = 309$) converges to a smooth solution with a minimal strain above the threshold -1.16 . For the simulation with 1750 and 1800 vertices ($L/t = 1151$ and $L/t = 1184$), the minimal strain is sufficiently low to cross over the threshold value -1.16 and a sudden drop of the minimal strain is observed as a signature of the stress focusing dynamics. For the small sheet with $W/t_e = 35$ and $W/t_e = 49$, there is no buckling transition because the compression strain remains below the threshold $1.16 \times (t_e/W)$.

Figure 3 (d) represents the longitudinal spacing δ between the points of minimum strain. A value $\delta = 0$ means that there is a total of 2 local minima for the compression strain located on the mid-length line $u = 0$. With $\delta > 0$,

there are 4 local minima for the compression strain as shown in figure 3 (b). The number of local minima sets the profile of first buckling event. In the simulation with $1750 \times 470 \times 2$ vertices, the stress focusing is first triggered at the 4 symmetric points of maximal compression strain. But rapidly, the 4 points travel towards the mid-length line and an abrupt increase of the maximal compression is observed when the pairs of stress focusing points merge.

The transition to stress focusing identified in experiments and simulations can be rationalized by a toy model that minimizes the elastic energy of the self-contacted sheet and then verify if the buckling criterion identified in the simulations is satisfied. To estimate the elastic energy, we assume that the sheet at self-contact is described by its typical transverse curvature that takes the value $c_0 \sim 1/W$ at $u = 0$ and c_e at the free ends at $u = \pm L/2$. By considering only the first-order contributions, the total elastic energy scales as:

$$\frac{\mathcal{E}(c_e)}{ELWt} \sim t^2(c_0^2 + c_e^2) + t^2 \frac{W^4}{L^4}(c_0 - c_e)^2 + \frac{W^8(c_0 - c_e)^4}{L^4} \quad (1)$$

with E the Young modulus. The terms in the right hand-side stand for the transverse bending energy, the longitudinal bending energy and the longitudinal stretching energy (see supplemental material). c_e is the only free parameter of the model and its value is obtained by the minimization of the energy $\partial \mathcal{E}(c_e)/\partial c_e = 0$ that yields to:

$$t^2 c_e - t^2 \frac{W^4}{L^4}(c_0 - c_e) - 2 \frac{W^8(c_0 - c_e)^3}{L^4} = 0 \quad (2)$$

Although an analytical solution for equation (2) exists from Cardano's formula (see supplemental material), we restrict the discussion for simplicity here to the highly-elongated sheets with $L^4 \gg W^4$. In this regime, the second term corresponding to the longitudinal bending is negligible. If we approximate the first term to t^2/W^2 , the scaling for the curvature is $c_0 - c_e \sim t^{2/3}L^{4/3}/W^3$. According to our previous work[30], the scaling for the stretching induced by a transverse bending is $\epsilon_{uu} \sim W^4 c'^2$ in which $c' \sim (c_0 - c_e)/L$. The criterion $|\epsilon_{uu}|(W_c/t) \sim 1$ identified from the simulations takes the form $W_c \sim t^{1/3}L_c^{2/3}$.

The exact solution of equation (2) shows that the scaling $W_c \sim t^{1/3}L^{2/3}$ is valid only for large W/t for which W^4/L^4 is consistently negligible. This exact solution also predicts an absence of buckling transition for small W/t as found in the simulations. Finally, the agreement between the experiments and the scaling relation with the exponent $2/3$ in figure 2 is consistently better for the transition in the region with large W/t .

The present results have evidenced a simple scaling relationship for the critical compressive strain of a sheet buckling with stress focusing, that is $\epsilon_c \sim t/W$ with a prefactor close to unity, as shown in figure 3(c) and consistently with the toy model. In our previous work[30],

the existence of a longitudinal compression for a transversely curved sheet was proposed to satisfy internal mechanical equilibrium in a model. Its relevance was only justified indirectly via a detailed analysis of the persistence length. Here, we show that the induced compression strain has a physical meaning and it acts equivalently than an external compression load applied to a curved plate: the scaling relationship $\epsilon_c \sim t/W$ is reminiscent of the classical buckling of cylindrical shells, where linear stability analysis predicts $\epsilon_c = 1/\sqrt{3(1-\nu^2)} \times t/R$ [42], with ν denoting the Poisson coefficient of the shell and R its radius of curvature. Notably, the above-mentioned formula infamously overestimates the buckling load of cylindrical and spherical shells [43], because those systems are extremely imperfection-sensitive [44, 45]. This affects the reliability of thin shell structures, even for precisely manufactured shells such as soda cans [46] and space rockets [43]. In contrast, the present work shows that the predicted and experimental buckling thresholds of a thin sheet submitted to pure bending are in agreement, as reported in figure 2. This hints that the present system is relatively insensitive to imperfections, which provides an interesting future route to reliably control buckling events in functional and smart materials. For example, with the buckling transition characterized here, it is possible to design fast-moving passive materials under external perturbations by choosing appropriate sheets dimensions to sit close to the buckling transition.

-
- [1] Lord Rayleigh, “On the bending and vibration of thin elastic shells, especially of cylindrical form,” *Proceedings of the Royal Society of London* **45**, 105–123 (1888).
- [2] Thomas A Witten, “Stress focusing in elastic sheets,” *Reviews of Modern Physics* **79**, 643 (2007).
- [3] Enrique Cerda and L Mahadevan, “Conical surfaces and crescent singularities in crumpled sheets,” *Physical Review Letters* **80**, 2358 (1998).
- [4] Sahraoui Chaïeb, Francisco Melo, and Jean-Christophe G eminard, “Experimental study of developable cones,” *Physical review letters* **80**, 2354 (1998).
- [5] Enrique Cerda, Sahraoui Chaieb, Francisco Melo, and L Mahadevan, “Conical dislocations in crumpling,” *Nature* **401**, 46–49 (1999).
- [6] M Ben Amar and Y Pomeau, “Crumpled paper,” *Proceedings of the Royal Society of London. Series A: Mathematical, Physical and Engineering Sciences* **453**, 729–755 (1997).
- [7] Alex Lobkovsky, Sharon Gentges, Hao Li, David Morse, and Thomas A Witten, “Scaling properties of stretching ridges in a crumpled elastic sheet,” *Science* **270**, 1482–1485 (1995).
- [8] Eric Sultan and Arezki Boudaoud, “Statistics of crumpled paper,” *Physical review letters* **96**, 136103 (2006).
- [9] Christian Andr e Andresen, Alex Hansen, and Jean Schmittbuhl, “Ridge network in crumpled paper,” *Physical review E* **76**, 026108 (2007).
- [10] Alexander S Balankin, Didier Samayoa Ochoa, Israel Andr es Miguel, Juli an Pati no Ortiz, and Miguel  ngel Mart nez Cruz, “Fractal topology of hand-crumpled paper,” *Physical Review E* **81**, 061126 (2010).
- [11] Anne Dominique Cambou and Narayanan Menon, “Three-dimensional structure of a sheet crumpled into a ball,” *Proceedings of the National Academy of Sciences* **108**, 14741–14745 (2011).
- [12] Andrew B Croll, Timothy Twohig, and Theresa Elder, “The compressive strength of crumpled matter,” *Nature communications* **10**, 1–8 (2019).
- [13] Omer Gottesman, Efi Efrati, and Shmuel M Rubinstein, “Furrows in the wake of propagating d-cones,” *Nature communications* **6**, 1–7 (2015).
- [14] Julien Chopin and Arshad Kudrolli, “Disclinations, e-cones, and their interactions in extensible sheets,” *Soft Matter* **12**, 4457–4462 (2016).
- [15] John A Rogers and Yonggang Huang, “A curvy, stretchy future for electronics,” *Proceedings of the National Academy of Sciences* **106**, 10875–10876 (2009).
- [16] Jiayan Luo, Hee Dong Jang, Tao Sun, Li Xiao, Zhen He, Alexandros P Katsoulidis, Mercouri G Kanatzidis, J Murray Gibson, and Jiaying Huang, “Compression and aggregation-resistant particles of crumpled soft sheets,” *ACS nano* **5**, 8943–8949 (2011).
- [17] Shun Mao, Zhenhai Wen, Haejune Kim, Ganhua Lu, Patrick Hurley, and Junhong Chen, “A general approach to one-pot fabrication of crumpled graphene-based nanohybrids for energy applications,” *ACS nano* **6**, 7505–7513 (2012).
- [18] Xiaofei Ma, Michael R Zachariah, and Christopher D Zangmeister, “Crumpled nanopaper from graphene oxide,” *Nano letters* **12**, 486–489 (2012).
- [19] Wei Yan, Wen-Yu He, Zhao-Dong Chu, Mengxi Liu, Lan Meng, Rui-Fen Dou, Yanfeng Zhang, Zhongfan Liu, Jia-Cai Nie, and Lin He, “Strain and curvature induced evolution of electronic band structures in twisted graphene bilayer,” *Nature communications* **4**, 1–7 (2013).
- [20] Pedro M Reis, “A perspective on the revival of structural (in) stability with novel opportunities for function: from buckliphobia to buckliphilia,” *Journal of Applied Mechanics* **82** (2015).
- [21] Douglas P Holmes, “Elasticity and stability of shape changing structures,” *Current opinion in colloid & interface science* (2019).
- [22] Robert D Schroll, Eleni Katifori, and Benny Davidovitch, “Elastic building blocks for confined sheets,” *Physical review letters* **106**, 074301 (2011).
- [23] JF Fuentealba, O Albarr n, E Hamm, and E Cerda, “Transition from isometric to stretching ridges in thin elastic films,” *Physical Review E* **91**, 032407 (2015).
- [24] Arezki Boudaoud, Pedro Patr cio, Yves Couder, and Martine Ben Amar, “Dynamics of singularities in a constrained elastic plate,” *Nature* **407**, 718–720 (2000).
- [25] Beno t Roman and Alain Pocheau, “Stress defocusing in anisotropic compaction of thin sheets,” *Physical review letters* **108**, 074301 (2012).
- [26] Enrique Cerda, Lakshminarayanan Mahadevan, and Jos e Miguel Pasini, “The elements of draping,” *Proceedings of the National Academy of Sciences* **101**, 1806–1810 (2004).
- [27] Alexander E Lobkovsky and TA Witten, “Properties of ridges in elastic membranes,” *Physical Review E* **55**, 1577 (1997).

- [28] Enrique Cerda and Lakshminarayanan Mahadevan, “Geometry and physics of wrinkling,” *Physical review letters* **90**, 074302 (2003).
- [29] Hugues Vandeparre, Miguel Piñeirua, Fabian Brau, Benoit Roman, José Bico, Cyprien Gay, Wenzhong Bao, Chun Ning Lau, Pedro M Reis, and Pascal Damman, “Wrinkling hierarchy in constrained thin sheets from suspended graphene to curtains,” *Physical Review Letters* **106**, 224301 (2011).
- [30] Thomas Barois, Loïc Tadrast, Catherine Quilliet, and Yoël Forterre, “How a curved elastic strip opens,” *Physical review letters* **113**, 214301 (2014).
- [31] Valerio Pini, JJ Ruz, Priscila M Kosaka, O Malvar, Montserrat Calleja, and J Tamayo, “How two-dimensional bending can extraordinarily stiffen thin sheets,” *Scientific reports* **6**, 1–6 (2016).
- [32] Daichi Matsumoto, Tomohiko G Sano, and Hirofumi Wada, “Pinching an open cylindrical shell: Extended deformation and its persistence,” *EPL (Europhysics Letters)* **123**, 14001 (2018).
- [33] Matteo Taffetani, Finn Box, Arthur Neveu, and Dominic Vella, “Limitations of curvature-induced rigidity: How a curved strip buckles under gravity,” *EPL (Europhysics Letters)* **127**, 14001 (2019).
- [34] Basile Audoly and Yves Pomeau, “Elasticity and geometry: from hair curls to the non-linear response of shells,” (2010).
- [35] Eric M Kramer and Thomas A Witten, “Stress condensation in crushed elastic manifolds,” *Physical Review Letters* **78**, 1303 (1997).
- [36] Hyunjune Sebastian Seung and David R Nelson, “Defects in flexible membranes with crystalline order,” *Physical Review A* **38**, 1005 (1988).
- [37] WA Curtin and H Scher, “Mechanics modeling using a spring network,” *Journal of Materials Research* **5**, 554–562 (1990).
- [38] Martin Ostoja-Starzewski, “Lattice models in micromechanics,” *Appl. Mech. Rev.* **55**, 35–60 (2002).
- [39] T Omori, T Ishikawa, D Barthès-Biesel, A-V Salsac, J Walter, Y Imai, and T Yamaguchi, “Comparison between spring network models and continuum constitutive laws: Application to the large deformation of a capsule in shear flow,” *Physical Review E* **83**, 041918 (2011).
- [40] Brian Anthony DiDonna, “Scaling of the buckling transition of ridges in thin sheets,” *Physical Review E* **66**, 016601 (2002).
- [41] Mikko Alava and Kaarlo Niskanen, “The physics of paper,” *Reports on progress in physics* **69**, 669 (2006).
- [42] John W Hutchinson, “Knockdown factors for buckling of cylindrical and spherical shells subject to reduced biaxial membrane stress,” *International Journal of Solids and Structures* **47**, 1443–1448 (2010).
- [43] Victor I Weingarten, P Seide, and JP Peterson, “Buckling of thin-walled circular cylinders,” *NASA SP-8007* (1968).
- [44] J Singer, J Arbocz, and T Weller, “Vol. 2, shells, built-up structures, composites and additional topics,” *Buckling Experiments: Experimental methods in buckling of thin-walled structures* (2002).
- [45] S Gerasimidis, E Viro, JW Hutchinson, and SM Rubinstein, “On establishing buckling knockdowns for imperfection-sensitive shell structures,” *Journal of Applied Mechanics* **85** (2018).
- [46] Emmanuel Viro, Tobias Kreilos, Tobias M Schneider, and Shmuel M Rubinstein, “Stability landscape of shell buckling,” *Physical review letters* **119**, 224101 (2017).